Analyzing Aircraft Surveillance Signal Quality at the 1090 Megahertz Radio Frequency

Sun, J.; Hoekstra, J.M.

Publication date
2020

Document Version
Final published version

Published in
ICRAT 2020

Analyzing Aircraft Surveillance Signal Quality at the 1090 Megahertz Radio Frequency

Junzi Sun*, Jacco M. Hoekstra†
Faculty of Aerospace Engineering,
Delft University of Technology,
Delft, the Netherlands
Email: *j.sun-1@tudelft.nl, †j.m.hoekstra@tudelft.nl

***Abstract*—Due to the increasing demands for real-time air traffic monitoring, the 1090 megahertz radio frequency has become the most utilized communication channel for aircraft surveillance purposes. Several services are using the radio frequency at the same time, which are Mode A/C communications and Mode S communications. These different types of communications are not coordinated, meaning that the quality of a communication channel can deteriorate with the increasing number of aircraft in the airspace. This deterioration may further worsen with the increasing number of aircraft that comply with the Automatic Dependent Surveillance-Broadcast requirement, which is implemented based on Mode S Extended Squitter.**

In this paper, we conduct experiments to determine the quality of 1090 megahertz radio frequency by analyzing the low-level signals using an open-source software-defined radio. First, we implement the demodulation of Mode A/C and Mode S signals from the raw in-phase and quadrature signals with a high sampling rate. Then, several methods are employed to study the occupancy of the communication channel and the garbling severity of the signals, as well as the error rate in ADS-B signals. All results show that the radio frequency is experiencing high communication load during day time air traffic operations. The results also suggest a need for a major redesign of the aircraft surveillance system in the future due to the current inefficient utilization of this radio frequency.

***Keywords* —** Aircraft surveillance, Communication, Signal analysis, Signal quality, 1090 megahertz, Mode S, ADS-B

I. Introduction

With the increasing air traffic demands in the last few decades, the 1090 megahertz (MHz) radio frequency has become one of the busiest telecommunication channels in the modern controlled airspace. Traditionally, this frequency was designed for aircraft transponders to comply with secondary surveillance radar interrogations. Before the 1980s, for civil aviation, the 1090 MHz frequency was used for Air Traffic Control Radar Beacon System (ATCRBS) Mode A/C communications, which allow the transponder to transmit identity (squawk code) and barometric altitude of the aircraft.

Due to the increase in air transportation, several design drawbacks of Mode A/C were shown. For instance, only a limited amount of information can be requested, and there are a very small number of identity codes exist, signal level issues such as false replies unsynchronized in time (FRUIT) and garbling also occur [1]. To address these problems, Mode S communication was proposed in the 1980s, which allowed the secondary surveillance radar to interrogate specific information from selected aircraft.

In the 2000s, a new Mode S capability, the Mode S Extended Squitter [2], was introduced to allow for the automatic broadcast of certain aircraft information without the need for interrogation. This was eventually adopted as the primary communication channel for Automatic Dependent Surveillance-Broadcast (ADS-B) services.[1] The implementation of ADS-B via the 1090 Extended Squitter has allowed for an enormous amount of flight data to be broadcast and received by air traffic controllers, as well as researchers around the world through low-cost off-the-shelf receivers, and inspired many studies [3], [4]. Studies conducted in [5], [6] made use of interrogations and responses from an experimental radar and showed the statistics of the different communications and the quality of communication in a certain part of the US airspace.

However, with the large quantitative of Mode S Extended Squitter signals, on top of Mode S responses, TCAS, and legacy Mode A/C responses, the 1090 MHz frequency is much busier nowadays, especially in European airspace. The degradation of the signal has become a non-negligible problem in many places. Several analyses were conducted to explore the quality of ADS-B or Mode S data [7], [8], [9], [10] based on decoded Mode S data. In our earlier research [11], we conducted a brief analysis of such degradation based on statistics of corrupted Mode S (including ADS-B) messages. However, these analyses did not paint a complete picture of communications on the 1090 MHz radio frequency, since they only dealt with a subset of Mode S signals.

The paper is focused on a multi-level analysis covering the low-level signals up to the decoded Mode-S data. In Figure 1, the scope of this paper is shown. First, we collect the In-phase and quadrature (I/Q) modulated signal from a software-defined radio (SDR) receiver. Then, the signals are demodulated and analyzed. The analyses include both Mode S (including ADS-B) signals and Mode A/C signals, as well as the power and corruption of ADS-B signals. Furthermore, decoded ADS-B information is also used to analyze the error characteristics of the data link.

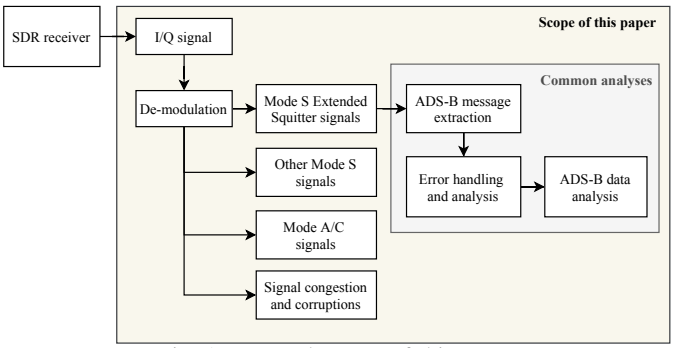

Fig. 1: Research scope of this paper

[1] Alternative channels for ADS-B are Universal Access Transceiver (UAT) via the 978 MHz radio frequency and VHF Data Link Mode 4 (VDL4) via the 108-137 MHz VHF frequency band. However, neither of these two solutions were adopted widely, meaning that almost all ADS-B communications nowadays are transmitted on the 1090 MHz radio frequency channel.

The main research objective of this paper is to analyze the utilization and quality of the 1090 MHz radio frequency in busy airspace where the traffic density is high and multiple aircraft surveillance services are used. Our goals are to find out whether the data link has been sufficiently utilized and how severe the congestion is during the different hours of the air traffic operations.

The other main research focus of this paper is to examine the severity of signal garbling. The concept of garbling refers to the overlapping of multiple signals. It is inherited from Mode A/C communication and has gotten worse in the modern 1090 MHz radio frequency, where different aforementioned surveillance services are implemented.

For the experiments in this paper, we use a large quality of raw signal data collected by our 1090 MHz receiver located in the Netherlands, which provides a common coverage radius of more than 200 kilometers. There is a major European airport, Amsterdam Airport Schiphol (EHAM), which is located within the range of the receiver. Hence a large amount of air traffic can be observed. In addition to arriving and departing flight from EHAM, we also observe a large amount of cruise flight within the Maastricht Upper Area Control Centre (MUAC) airspace. The significance of this data set is that it contains the low-level raw signal that can be used to construct the exact radio environment of the 1090 MHz frequency. Based on this data set and several novel methods proposed in this paper, we can perform the multi-level analyses shown in Figure 1. To accomplish the analysis, we develop a pipeline that allows the raw signals to be demodulated, decoded, and analyzed at different stages.

The remainder of the paper is structured as follows. Section two describes the fundamentals of the communications transmitted via the 1090 MHz radio frequency. Section three introduces the pipeline of how signals are processed using a software-defined radio device. Section four discusses methodologies for different analyses conducted in this paper. Section five presents the analysis results. Finally, discussion and conclusions are presented in sections six and seven.

II. Signals of the 1090 MHz radio frequency

A. Mode A/C

Mode A/C are ATCRBS surveillance methods adopted from the military system, which had been used since World War II. Mode A provides the identity of the aircraft, while Mode C provides the altitude of the aircraft. The signal is modulated using On-Off Keying (OOK), which is the most simple form of the amplitude-shift keying (ASK) modulation. Using OOK, bit value 1 is represented by the presence of the carrier signal, while bit value 0 is represented by the absence of the carrier signal. The structures for both Mode A and Mode C responses are transmitted in the same format, which is shown in Figure 2.

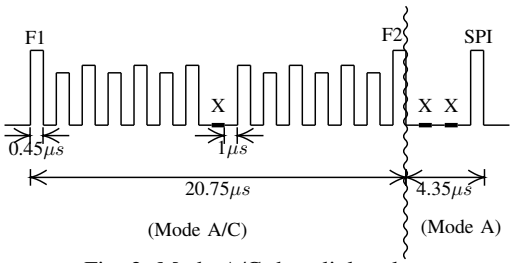

Fig. 2: Mode A/C downlink pulses

All pulses last for 0.45 microseconds, and the gap between two possible pulses is a 1 microsecond. The entire response lasts for 20.75 microseconds, which starts and ends with the bit 1 (F1 and F2 pulses). The pulse in the center of the response is always absent. Pulses between F1 and F2 can either be present or absent, representing the 1 or 0. For identity replies, the Special Purpose Identification (SPI) pulse may be added (through voice communication command) for certain aircraft, which allows their identity to be confirmed by air traffic controllers. Knowing the reply type, the identity or altitude can be decoded as the octal squawk code or Gray code [12].

Mode A/C communication is designed so that all aircraft can respond to any interrogations from any Mode A/C surveillance radar at the same time. Hence, a third-party observer cannot tell whether a reply corresponds to a Mode A or Mode C interrogation. Several limitations of the ATCRBS system were shown with the increasing air traffic in the 1980s [13], such as a limited number of squawk codes, FRUIT, azimuth inaccuracy, and over-interrogation. But the most significant impact of Mode A/C responses to 1090 MHz radio frequency is garbling, which refers to the situation where two messages overlap with each other. Modeling and analyzing the garbling effect is one of the main goals in later sections of this paper.

B. Mode S

Mode S was designed to overcome many of the limitations in Mode A/C communication. It makes use of the 24 bits transponder address to distinguish messages from different aircraft, which in theory would support 2^{24} (more than 16 million) unique aircraft. The main characteristic of Mode S is the selective interrogation, which drastically reduces the amount of signal garbling and FRUIT comparing to Mode A/C. It also uses longer messages that allow for more information to be transmitted by aircraft.

The uplink and downlink of Mode S use different frequencies and modulation methods. The uplink (1030 MHz) uses modern Differential Phase-Shift Keying (DPSK) modulation, which is significantly more advanced than other candidate modulations [14]. The downlink was designed to use the Pulse Position Modulation (PPM), which is a compromise between noise performance and cost-effectiveness. However, the choice of adopting pulse modulation rather than phase modulation in downlink has significantly contributed to the interference effect caused by the FRUIT of signals.

In Figure 3, an example of downlink pulses of Mode S is illustrated. All Mode S replies start with a preamble pulse representing `1010000101000000` and follow by the message data that is modulated using the pulse position modulation as shown in the figure.

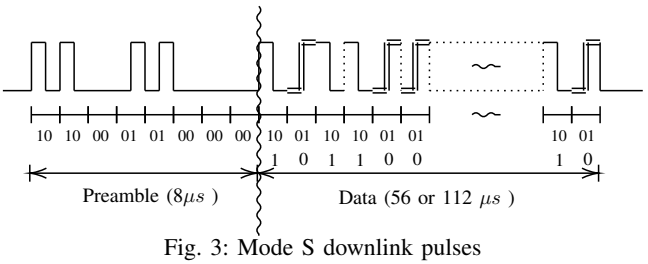

Fig. 3: Mode S downlink pulses

Mode S supports different types of information exchanged and identified by the uplink (or downlink) format code. Currently, 11 out of 24 downlink format (DF) codes are defined and implemented. Among these existing 11 downlink format codes, codes 17, 18, and 19 are defined as the Mode S Extended Squitter. These messages are broadcast automatically without the need for SSR interrogation.

For other interrogation based formats, code 11 (all-call reply) is used by secondary surveillance radar to discover aircraft in its airspace. Codes 4 and 5 are for short interrogations and replies that provide similar functionalities as Mode A/C. Codes 20 and 21 are long interrogations and replies that support up to 255 different types of information exchange. Codes 0 and 16 are used for ACAS. Finally, code 24 is designed for extended length messages.

C. Mode S Extended Squitter

Mode S Extended Squitter has become the most adopted platform for ADS-B implementation. Unlike other types of Mode S commu-

nications that reply to the interrogation of secondary surveillance radar, the extended squitter mode allows information to be broadcast without being interrogated. Studies from the OpenSky network [15] have shown that the amount of ADS-B messages account for 18 percent of all Mode S communications. It also found that there are more ADS-B messages than all other types of long Mode S replies (112-bit messages) combined. According to [2], the nominal broadcast rate of difference message types are defined as shown in Table I.

TABLE I: ADS-B Message rate for Mode-S Extended Squitter

Message type	Type code	Message rate
Surface position	5-8	2 per second
Airborne position	9-18, 20-22	2 per second
Velocity	19	2 per second
Identification	1-4	0.2 per second
Operational status	31	0.4 per second
Target state	29	0.8 per second
Total	all	5.4 per second

On average, each aircraft automatically broadcasts around five ADS-B messages each second. Since each message lasts about 120 μs, the amount of communication time needed for ADS-B is around 650 μs per aircraft per second, which converts to approximately 0.065% of the channel occupancy. Hence, in theory, if a perfect coordination condition would exist, the communication channel could only allow a maximum of around 1500 aircraft to transmit only ADS-B signals without overlapping. [2] However, since ADS-B communications are not coordinated and there is a much larger number of other types of Mode S and Mode A/C communications using the same radio frequency, signal collisions are determined to be more frequent. Furthermore, as some unmanned areal vehicles are also starting to make use of ADS-B transponder [16], the limitation can be reached very easily.

III. Signal Processing

In this section, we design a pipeline allowing raw signals, collected from a software-defined radio, to be processed. The pipeline includes the demodulation of samples, the extraction of Mode A/C and Mode S signals, the decoding of the Mode S content, and the analysis of these signals.

A. Demodulating and extracting signals

Most software-defined radio receivers provide the sampled signals in the in-phase and quadrature (I/Q) format. The I/Q format signal is a complex signal that can be translated into the amplitude and phase of the original signal at each sample point.

Both Mode A/C and Mode S downlink signals are modulated using ASK. Thus, knowing only the amplitude of the signal would allow the original signal to be sufficiently demodulated. The magnitude of received signals at each sampling point by the receiver can be calculated as:

$$A = \sqrt{I^2 + Q^2} \tag{1}$$

where I and Q are the in-phase and quadrature components of the signal, corresponding to the real and imaginary parts of the complex number. Based on signal amplitude from the I/Q data, we first employ a naive method to detect the noise floor. To do so, we make use of a short segment of a signal at the start of the stream. We split the stream into windows of 20 microseconds.[3] The noise floor is identified as the minimum mean amplitude of the windows:

$$A_{\text{noise}} = \min\{\bar{A}_1, \bar{A}_2, \cdots, \bar{A}_N\} \tag{2}$$

where $\bar{A}_i$ is the mean signal amplitude of a 20 μs window.

Once the noise floor amplitude is identified, we can extract signal segments by determining the length of the noise duration of noise between consecutive pulses. In this paper's experiment, we set the threshold of noise duration to 26 microseconds, which is approximately the maximum length of a Mode A signal.

When processing radio signals, it is also common to represent the signal power or amplitude in terms of decibel (dB). The following relationship between amplitude ratio and decibel is used throughout the rest of this paper.

$$\begin{aligned} L &= 20\log_{10}\left(\frac{A}{A_0}\right) \quad \text{(dB)} \\ &= 10\log_{10}\left(\frac{P}{P_0}\right) \quad \text{(dB)} \end{aligned} \tag{3}$$

where A and P are amplitude and power of the signal.[4] A_0 and P_0 are amplitude and power of the reference signal, which often refers to the noise in this paper.

B. Signal decoding

By examine the length and the presence of the preamble of a signal, we can determine whether the signal is a Mode A/C or Mode S signal. In Figures 4, an example Mode A/C message is shown. The presence and absence of the carrier signal representing 1 and 0 are also shown in the figure. It is not possible to determine whether the altitude or identity code is interrogated here. However, in this paper, for signal analysis, we do not have to distinguish them.

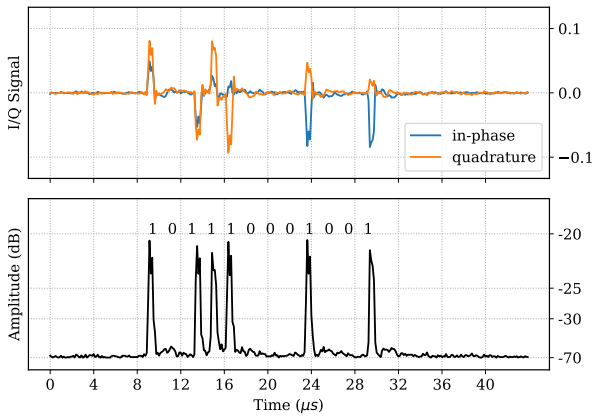

Fig. 4: An example of Mode A/C downlink signal

Mode S signals follow a well-defined structure. Hence, they can be thoroughly analyzed. In Figure 5, a short Mode S signal example is shown. After the end of the preamble, at around 10 μs in this sample, information is modulated using PPM and can be obtained conveniently according to the process shown in Figure 3.

C. Error detection

Understanding error patterns is one of the most important factors when analyzing the data link of 1090 MHz frequency communications. The primary reasons for the occurrence of errors are signal garbling and noise. Errors due to garbling are apparent since they distort signals. Errors caused by noise mostly affect aircraft that are located far from the receiver, since the signal to noise ratio decreases with increasing distance to the receiver.

[2] For reference, with our receiver, it is already common to observe more than 250 aircraft simultaneously currently.

[3] 20 μs is empirically chosen, which is similar to the length of Mode A/C message.

[4] P is proportional to the A^2 of the signal.

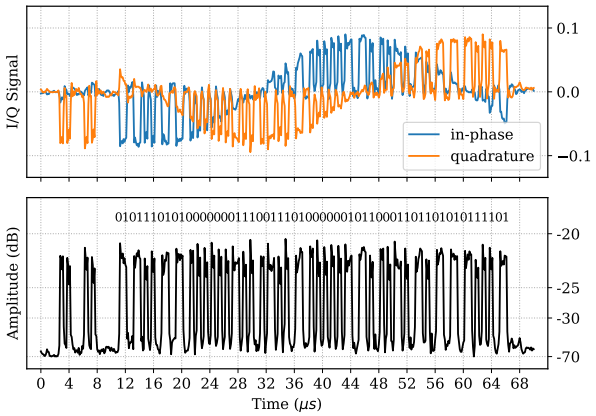

Fig. 5: An example of Mode S downlink signal

There is no easy way to perform Mode A/C error detection since such a mechanism was not introduced in the design of the ATCRBS system. However, in Mode S, mechanisms are implemented allowing for the detection and correction of error messages.

Mode S uses a cyclic redundancy check (CRC) algorithm [17] to detect (and potentially to correct) errors in messages. CRC is based on polynomial division over the finite field (or Galois field GF(2)), where the arithmetic operations wrap around the polynomial coefficient (either 1 or 0). The denominator, also knows as *generator*, used for Mode S CRC encoding and decoding is designated as:

$$\begin{aligned} G(x) = x^{24} + x^{23} + x^{22} + x^{21} + x^{20} + x^{19} \\ + x^{18} + x^{17} + x^{16} + x^{15} + x^{14} \\ + x^{13} + x^{12} + x^{10} + x^3 + 1 \end{aligned} \tag{4}$$

which is expressed as `1111111111111010000001001` in binary format. Bits representing the Mode S message (88 bits or 33 bits) can also be written in the polynomial format of the highest order (87 for long messages or 32 for short messages). Let x^i represent each bit of the message and $M(x)$ represent the polynomial corresponding Mode S message, the CRC reminder (parity) $P(x)$ can thus be calculated as:

$$\begin{aligned} M(x) &= \sum_{i=0}^{87 \text{ or } 32} a_i x^i, \quad a_i \in (0,1) \\ P(x) &= M(x) \ \% \ G(x) \end{aligned} \tag{5}$$

For an ADS-B message, $P(x)$ is directly transmitted as the parity in the last 24 bits of the message. Errors can be detected by performing the same computation process at the receiving side when received parity differs from this newly computed reminder.

However, for other types of Mode S messages, the final parity included in the message is not $P(x)$. Instead, a new parity $P_A(x)$ is calculated as:

$$P_A(x) = P(x) + A(x) \tag{6}$$

where $A(x)$ is the polynomial representing the ICAO address of the transponder. Since the interrogations are not known, information such as the transponder address is not known to third party receivers. The lack of this information makes error detection difficult. Hence, in this paper, we focus on using the existing error detection mechanism in ADS-B to analyze the error characteristics of the signals.

IV. Data Link Analysis

A. Activity factor

The activity factor (γ) defines the occupancy of the communication channel. It is calculated as the percentage of time when communications occur during a certain period:

$$\gamma = \frac{\sum_{i=1}^{n} \Delta t_i}{\Delta t} \tag{7}$$

where $\sum_{i=1}^{n} \Delta t_i$ is the sum of all active communication times and Δt is the total time period. A higher γ value indicates a higher channel occupancy, while a low γ indicates the under-utilization of the data link resource.

In the case of Mode S, high occupancy is correlated with a high probability of errors, since the communications are not coordinated. This is especially true for automatic broadcast services such as ADS-B. While performing the analysis of 1090 MHz frequency, the relationship between activity factor and error rate is an important aspect to be studied.

To correctly model the activity factor, we also need to accurately measure the active slots (Δt_i). An active slot can be defined in two different ways. Firstly, we can consider time intervals including all signals above the noise floor, denoted as Δt_∞. In this case, we are considering all radio visible aircraft. Secondly, we can consider only the time intervals including signals over a certain signal-to-noise ratio to be an active slot. This type of active slot is denoted as $\Delta t_{\text{snr}>x}$, where x represent signal to noise power in dB. Consequently, we have two different types of activity factors that can be calculated as:

$$\begin{aligned} \gamma_\infty &= \frac{\sum_{i=1}^{n} \Delta t_{\infty,i}}{\Delta t} \\ \gamma_{\text{snr}>x} &= \frac{\sum_{i=1}^{m} \Delta t_{\text{snr}>x,i}}{\Delta t} \end{aligned} \tag{8}$$

B. Garbling identification

Garbling refers to the phenomena where segments from two unsynchronized transmissions overlap with each other. Since there are often a large number of aircraft in busy airspace transmitting unsynchronized messages such as ADS-B and replies to different secondary radars, garbling is one of the main causes of errors in received messages. In Figures 6 and 7, two examples show different types of information loss due to garbling. In Figure 6, garbling between two Mode A/C messages is shown, while in Figure 7, the garbling between one Mode A/C message and one Mode S message is shown. In both cases, part of the information in the signal with lower power is lost.

To identify signal garbling, we propose a model based on signal energy in this paper. In summary, this model measures the variance in energy in pulses, and detects the garbling if the variance exceeds a threshold. To do so, we first normalize the amplitude of the signal to:

$$\boldsymbol{A}' = \frac{\boldsymbol{A}}{\max(\boldsymbol{A})} \tag{9}$$

Then, we obtain the subset of time series data where amplitudes are larger than the 70th percentile value of the signal amplitudes (denoted as $\boldsymbol{A}'_{\eta>.70}$). This allows us to obtain the peaks of the signal segment. And the garbling is determined when the following condition is met:

$$1 - \min(\boldsymbol{A}'_{\eta>.70}) > 0.3 \tag{10}$$

where the occurrence of garbling can be identified if the variation in normalized amplitude exceeds 30%. The results of this detection modeling applied to the example (garbled) signals from earlier are illustrated in Figure 8. As a comparison, the result of this detection modeling applied to a (non-garbled) signal from the earlier section is shown in Figure 9.

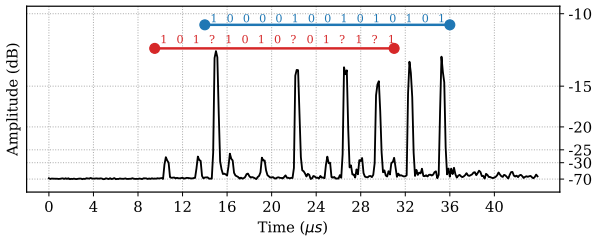

Fig. 6: An example of signal garbling between two Mode A/C messages

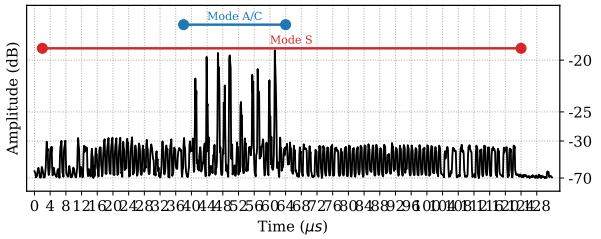

Fig. 7: An example of signal garbling between a Mode A/C message and a Mode S message

C. Signal power range modeling

Like other radio communications, the free-space loss of Mode S signal also follows the Friis transmission model, which states that the received signal power is in relationship with several factors of the transmitter and receiver as follows:

$$\frac{P_r}{P_t} = D_t D_r \left(\frac{\lambda}{4\pi d}\right)^2 \tag{11}$$

where P_r and P_t are power received and power transmitted. D_r and D_t are directivities related to the receiving and transmitting antenna. λ is the wavelength of the signal. d is the distance between the transmitter and receiver, and can be calculated based on the aircraft location reported in ADS-B messages. D_r and λ can be assumed constant for a fixed omnidirectional receiver. D_t is generally constant for a specific aircraft type. P_t and d are the only two parameters that define the received signal strength. However, since the transmission power is relatively constant for the same transponder,[5] the most significant variable that determines the receiving signal power is the distance. At the receiver side, the strength is measured by the relative amplitude of the demodulated signal. We can construct the following model to express the relationship between distance and received signal strength in decibel.

$$L_r = k - 20\log_{10} d \quad \text{(dB)} \tag{12}$$

where k is a parameter introduced to replace the constant terms. The final goal of this equation is to establish the power range model that is specific for each receiver setup.

V. Experiments and Results

A large quantity of raw signals is collected by an antenna located at the Delft University of Technology, which provides maximum coverage for more than 400 kilometers. However, due to free-space path loss, the majority of the signals are from the areas within the 200 kilometers of the radius to the receiver.

The software-defined receiver used for collecting raw signal is an open-source LimeSDR receiver, which supports up to 64 million samples per second. However, to limit the amount of data storage, we configure the sampling rate at eight million samples. This accounts for approximately four samples for each Mode S pulses. Even at this lower sampling rate, the raw IQ data is still extremely large (approximately four Gigabytes per minute), which makes it impractical to save raw signals for an extended duration.

[5]In most cases, the peak transmission power of the Mode S transponder is defined according to the class of equipment [2].

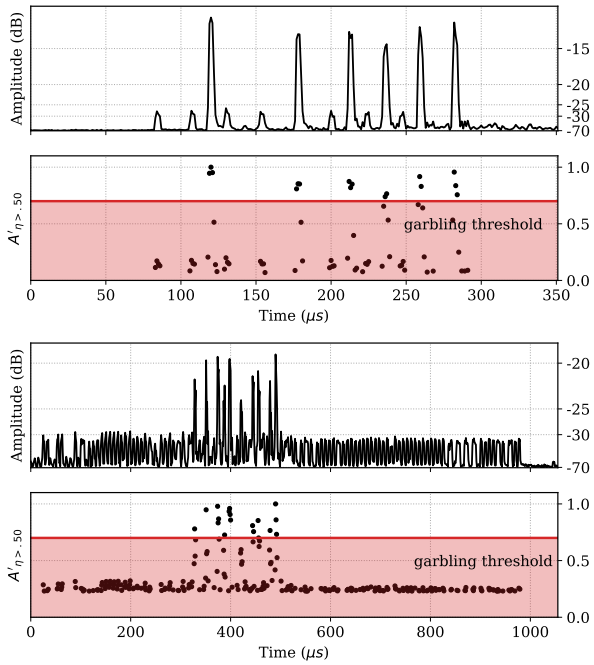

Fig. 8: Garbling detected, primary signals appear in the red threshold area.

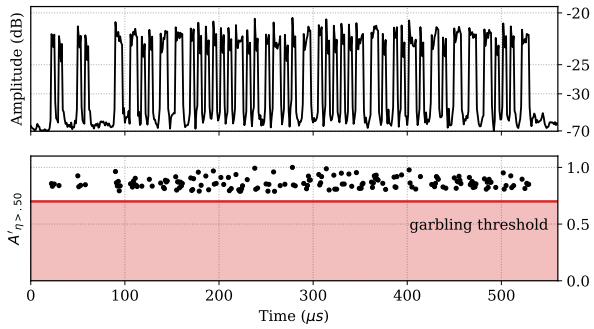

Fig. 9: Garbling not detected, no primary signal appears in the red threshold area.

Hence, for the experiments of this paper, we obtain a number of 30-second segments of the raw signal at each half-hour during a 24-hour period, which summarizes to around 100 Gigabytes of data in total. In Figure 10, the aircraft positions over these 24 hours are illustrated over the geographical region of the experiment. We can see that the majority of the signals are within the Dutch airspace.

A. Data link activity factor

Based on the collected data, the first analysis is designed to investigate the activity factor on the 1090 MHz radio frequency. The activity factory (Equation 8) measures the channel occupancy over the time, given a defined signal to noise power ratio. In Figure 11, different activity factor profiles based one different signal to noise power ratios are calculated over the 24-hour period.

Eight profiles illustrated in the figure correspond to different levels of signal to noise power ratios ranging from 5 dB to 20 dB. We can observe that there is a distinct difference regarding the radio

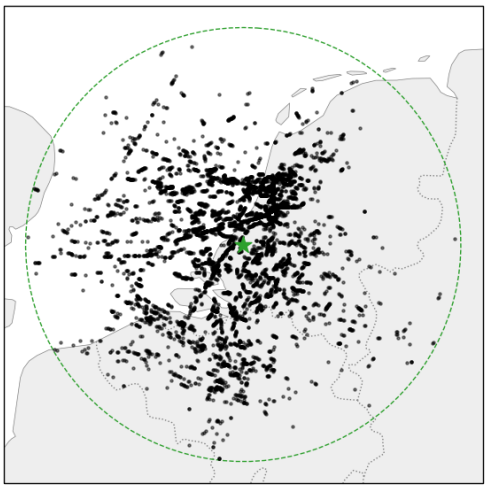

Fig. 10: Aircraft locations of over a 24-hour period and within 200 km radius of the receiver, consist of a 30-second sample sets at each half hour. The receiver is located at the center of the graph, and the circle indicates a 200 kilometers radius around the receiver.

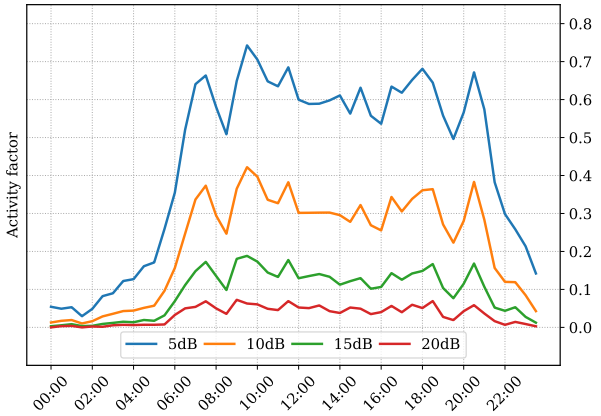

Fig. 11: Channel occupancy measured by activity factor over a period of 24 hours on 29 January, 2020. Different lines represent different signal to noise ratio thresholds in decibel.

frequency occupancy over different hours of air traffic operations. During the day time, from 06:00 to 20:00 UTC (07:00 to 21:00 local time), the channel is highly utilized. For the rest of the analyses in this paper, we chose the 10 dB signal power to noise threshold. For this chosen threshold, the channel occupancy is around 30%.

B. Garbling

When the radio frequency channel is at a high occupancy rate, the garbling of the signal is likely to occur. It is certain that when the signal to noise ratio threshold is low (weak signals), garbling happens constantly, since we are considering more aircraft with the increasing radio range. In this analysis, we take a look at garbling severity among signals of more than 10 dB over the noise. In Figure 12, the garbling statistics over the 24 hours is illustrated.

In the top plot of this Figure, the black line shows the number of signals over time, and the red line indicates the number of signals with garbling detected. In the bottom plot, the percentages of signals with garbling over time are shown. We can see that during the day, the garbling rate stays relatively constant at around 30%. It is worth emphasizing that 10 dB signals considered in this analysis translate into around 3 times the amplitude over the noise based on Equation 3.

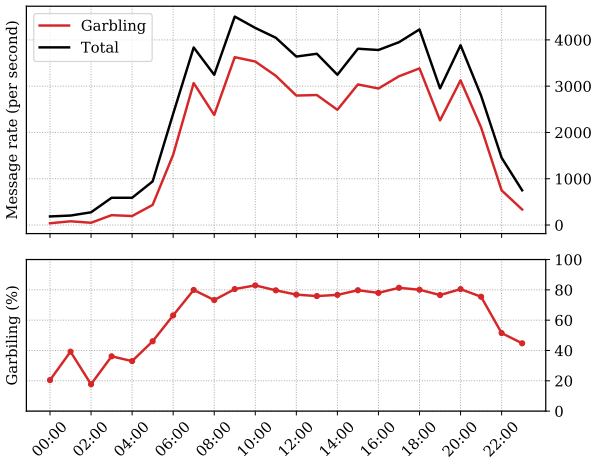

Fig. 12: Garbling rates during a 24 hour period on 29 January, 2020, including all signals 10dB above noise floor.

C. Mode A/C and Mode S statistics

In this analysis, we want to further separate signals according to their types, which are Mode A/C, Mode S short message, and Mode S long message. Mode S short and long messages can both be identified directly with the preamble pulse. We consider Mode A/C messages to have a duration between 20 and 26 μs, considering a potential SPI for Mode A messages. Signals of other lengths are marked as unknown messages type (e.g. due to overlapping of multiple signals). In Figure 13, the statistics regarding the distributions of the message rates of different types are shown. It is worth noting that determining Mode A/C based on messages length may not be as accurate as using preamble of Mode S messages.

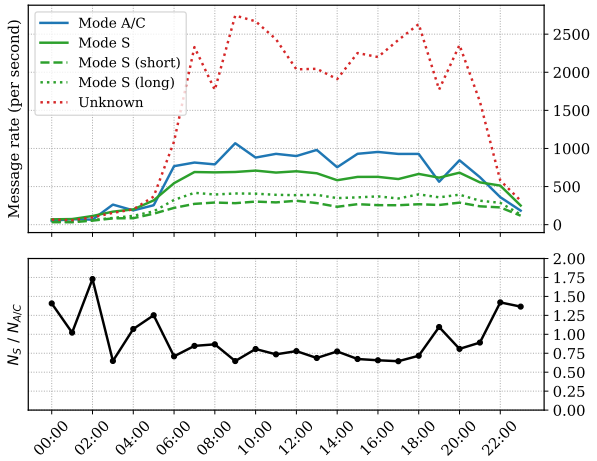

Fig. 13: Mode A/C and Mode S message rates during a 24 hour period on 29 January, 2020, including all signals 10dB above noise floor.

Next, examining only the Mode S messages, it is possible to discover the statistics regarding the types of Mode S interrogations that are been requested in our airspace. In Figure 14, we can see that the most interrogated downlink format is 11 (all-call reply), which is at a rate of 200 messages per second during the day time. Next, DF 20 (Comm-B altitude reply), DF 17 (Extended Squitter), DF 21 (Comm-B identity reply), and DF 4 (short altitude reply) are also common, with the message rate around 160, 110, 80, and 60 respectively. The least frequent messages are DF 5 (short identity reply) and DF 16 (ACAS), which are both less than 20 message per second.

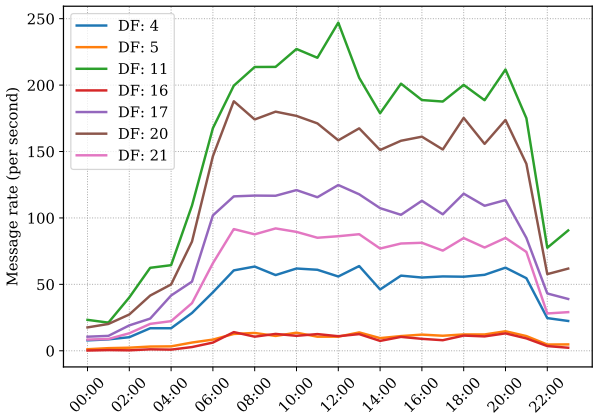

Fig. 14: Mode S message downlink format statistics during a 24 hour period on 29 January, 2020, including all signals 10dB above noise floor.

D. Mode S Extended Squitter

Correctness cannot be validated for all signals. However, ADS-B messages transmitted through Mode S Extended Squitter contain complete parity information, which allows us to examine the correctness of the ADS-B messages using Equation 5. Since the percentage of ADS-B messages can be assumed constant within a short period, by analyzing the error of ADS-B messages only, it is possible to indirectly infer the error rate of other types of Mode S long messages with the same length.

1) ADS-B Corruption rate: From all decoded Mode S messages, ADS-B messages (with downlink format 17) are extracted to perform the error detection. CRC check is applied to each ADS-B message. In Figure 15, the error rate, represented by the number of messages per second, is shown.

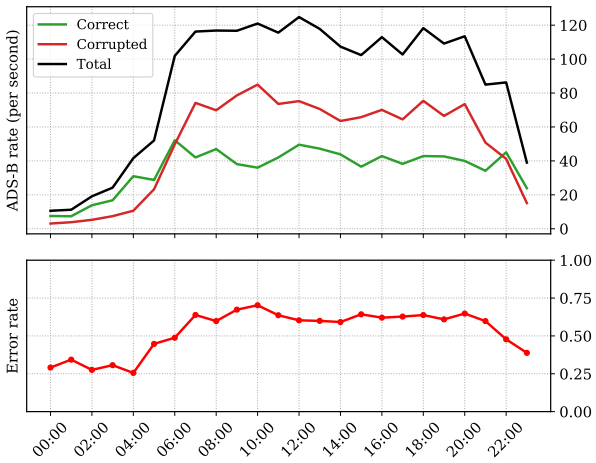

Fig. 15: Corruption detected in ADS-B messages during a 24 hour period on 29 January, 2020, including all signals 10dB above noise floor.

In the top plot of the figure, the black line indicates the total number of ADS-B messages detected over the period. The red line and green line represent the numbers of correct and corrupted messages respectively. The bottom plot of the figure shows the error rate, which is computed as the fraction of corrupted messages over the total number of messages.

We can see that the error rate is constantly over 25%, even during the night time operation period. During day time, the error rate is between 60% and 75%. Even though the CRC mechanism in ADS-B allows a certain degree of error correction, the severity of the error rate is not negligible according to the figures from this analysis. The results also agree with the independent analysis using a different type of receiver from [11].

Using this subset of ADS-B data, we can also analyze the relationship between error rate and signal to noise power ratio at different time. Hence, we visualize the error rates grouped by signal to noise power ratio and hours of the day and show the results in Figure 16.

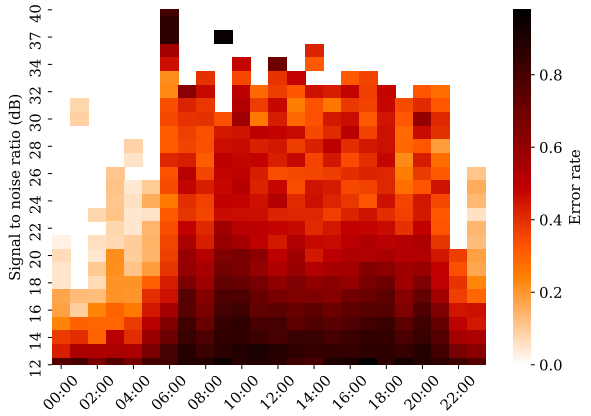

Fig. 16: Relationship between number of corrupted signals and signal power over a 24-hour period. The darker the shade of red, the higher the error rate under a specific signal power at a specific time. Showing only pairs with more than 20 messages.

In this figure, the horizontal axis shows the time of day, and the vertical axis shows the signal to noise ratio. The intensity of the shade indicates the severity of signal corruption. It is apparent that for weaker signals, the level of error rate is much higher during day time operations than during night time operations. This also suggests that a large portion of errors are caused by radio frequency congestion, rather than by the free-space loss of the signal. For signals over 35 dB, the error rate also becomes very high. This is likely because, in this power range, such signal strength can only be produced due to the overlapping of multiple signals.

2) Signal strength and range: In several previous analyses, we have discussed the relationships among message garbling, error, and signal power. Furthermore, ADS-B can provide us a better understanding of these parameters concerning the distance from the receiver. According to Equation 12, the signal power and distance model are constructed based on correct ADS-B position messages from the data. In the following Figure 17, the model is estimated and illustrated.

The density plot shows the relationship between signal power and distance of the aircraft to our receiver. The dashed line represents the model from Equation 12 fitted over the data.

VI. Discussion

A. Severity of data link congestion

All three analyses regarding data link activity factor (Figure 11), garbling rate (Figure 12), and error rate in ADS-B (Figure 16) have independently confirmed that the radio frequency has reached a level of over-utilization. During day time operations, the channel utilization is around 30% when considering signals that are stronger than 10dB above the noise. This translates to a range of approximately 200 km from the receiver.

When considering signals above 10 dB over the noise, we have also observed a garbling rate of around 80% among all types of messages, as well as an error rate of around 70% for ADS-B messages during the peak time of air traffic operations. In the dataset of this paper, the majority amount of the signals are within the around 150 km

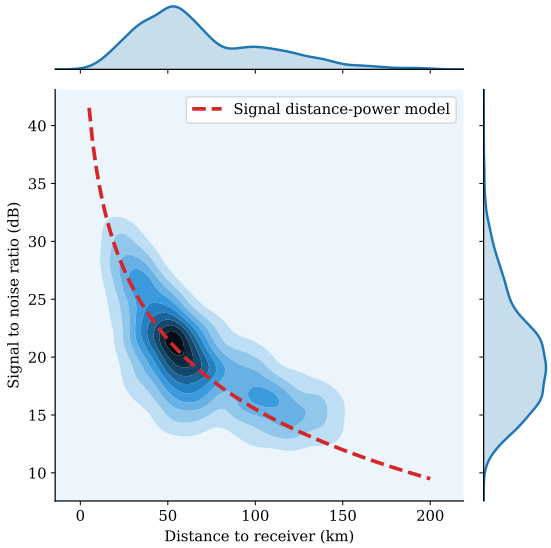

Fig. 17: Relationship between signal power and aircraft distance to receiver.

radius from the receiver according to Figure 17. When examining Figure 16, we can see that the error rate becomes less significant only when signal strength is more than 20 dB over the noise. However, this further reduces the range to approximately 50 km from the receiver in our scenario. These error rates may still be sufficient for current day applications, such as aircraft separation and conflict detection/resolution. But they could be a limiting factor for future use cases where unmanned aerial vehicles are involved.

B. Limitations

The data for this paper is gathered over 24 hours with a receiver located in the Netherlands. Thus, the situations described in this paper cannot represent the context globally. However, it can be considered as a reference for European airspace. The methods and analyses proposed in this paper can certainly be applied to any other airspace.

To reduce the data storage we only collected a 30-second sample per half hour. This can sometimes create a relatively large discontinuity between two consecutive time steps. This is another limitation in the dataset used in this paper.

The garbling detection method used in this paper can only identify the mix of multiple signals with different powers. For signals with the same power level, other information could be considered in the future, for example, the phase and duration of each signal.

We examine the relationship between signal power and distance to the receiver, as the mathematical model can capture the relationship clearly. However, there are still uncertainties in the fitted model. We suspect that the variance is caused by the assumption on the transponder transmission powers are constant. Transmission power likely differs among different aircraft. The model can be improved in the future by considering the variation of aircraft types.

VII. Conclusions

At the beginning of this paper, we proposed an investigation of the 1090 megahertz radio frequency usage due to high air traffic density and the increasing demand for aircraft surveillance. Throughout the paper, we have designed different analysis methods to examine the severity of the data link congestion. Different parameters have pointed out concerns regarding the quality of the radio frequency. We have found that even for promising surveillance technology like ADS-B, the error rate can be around 70% during day time operations. This situation is also likely to apply for other types of Mode S surveillance services.

Given this alarming situation for busy airspace like the case from this paper, as a short term recommendation, the amount of Mode A/C interrogation should be reduced where possible and replaced by adopting technologies like ADS-B since aircraft identity and altitude are already included in ADS-B. The long term solution may be a redesign of current data link protocols using the 1090 megahertz radio frequency. For example, a better modulation method that is more robust to interference would greatly increase the link quality. A better version of the Mode S protocol allowing messages to be decoded transparently could also reduce the number of interrogations from different air traffic controllers. These solutions may even allow interrogation of future unmanned aerial vehicles using the same communication frequency.

Acknowledgment

We would like to thank Petr Jonas from EUROCONTROL for the valuable feedback regarding the channel occupancy analysis and general comments for this paper.

References

[1] ICAO, *Secondary Surveillance Radar Mode S Advisory Circular*. International Civil Aviation Organization, 1983.

[2] RTCA, *Minimum Operational Performance Standards for 1090 MHz Extended Squitter: Automatic Dependent Surveillance-Broadcast (ADS-B) and Traffic Information Services-Broadcast (TIS-B)*. RTCA, 2006.

[3] M. Schäfer, M. Strohmeier, V. Lenders, I. Martinovic, and M. Wilhelm, "Bringing up opensky: A large-scale ads-b sensor network for research," in *Proceedings of the 13th international symposium on Information processing in sensor networks*, pp. 83–94, IEEE Press, 2014.

[4] J. Sun, J. Ellerbroek, and J. Hoekstra, "Flight Extraction and Phase Identification for Large Automatic Dependent Surveillance–Broadcast Datasets," *Journal of Aerospace Information Systems*, vol. 14, no. 10, pp. 566–571, 2017.

[5] A. Drumm, G. Harris, B. Chludzinski, W. Harman, and A. Panken, "Lincoln Laboratory 1030/1090 MHz Monitoring," tech. rep., MIT Lincoln Laboratory Project Report ATC-372, 2010.

[6] A. Panken, W. Harman, C. Rose, A. Drumm, B. Chludzinski, T. Elder, and T. Murphy, "Measurements of the 1030 and 1090 MHz environments at JFK international airport," tech. rep., MIT Lincoln Laboratory Project Report ATC-390, 2012.

[7] B. S. Ali, W. Schuster, W. Ochieng, and A. Majumdar, "Analysis of anomalies in ads-b and its gps data," *GPS solutions*, vol. 20, no. 3, pp. 429–438, 2016.

[8] T. Verbraak, J. Ellerbroek, J. Sun, and J. Hoekstra, "Large-scale ads-b data and signal quality analysis," in *12th USA/Europe Air Traffic Management Research and Development Seminar*, 2017.

[9] A. Tabassum, N. Allen, and W. Semke, "Ads-b message contents evaluation and breakdown of anomalies," in *2017 IEEE/AIAA 36th Digital Avionics Systems Conference (DASC)*, pp. 1–8, IEEE, 2017.

[10] M. Schäfer, M. Strohmeicr, M. Smith, M. Fuchs, V. Lenders, and I. Martinovic, "Opensky report 2018: assessing the integrity of crowdsourced mode s and ads-b data," in *2018 IEEE/AIAA 37th Digital Avionics Systems Conference (DASC)*, pp. 1–9, IEEE, 2018.

[11] J. Sun, H. Vû, J. Ellerbroek, and J. M. Hoekstra, "pymodes: Decoding mode-s surveillance data for open air transportation research," *IEEE Transactions on Intelligent Transportation Systems*, 2019.

[12] J. L. Gertz, "The atcrbs mode of dabs," tech. rep., MASSACHUSETTS INST OF TECH LEXINGTON LINCOLN LAB, 1977.

[13] V. A. Orlando, "The Mode S Beacon Radar System," *The Lincoln Laboratory Journal*, vol. 2, no. 3, pp. 345–362, 1989.

[14] T. J. Goblick, "Dabs modulation and coding design: A summary," tech. rep., 1976.

[15] M. Schäfer, X. Olive, M. Strohmeier, M. Smith, I. Martinovic, and V. Lenders, "Opensky report 2019: Analysing tcas in the real world using big data," in *2019 IEEE/AIAA 38th Digital Avionics Systems Conference (DASC)*, IEEE, September 2019.

[16] A. G. Foina, R. Sengupta, P. Lerchi, Z. Liu, and C. Krainer, "Drones in smart cities: Overcoming barriers through air traffic control research," in *2015 Workshop on Research, Education and Development of Unmanned Aerial Systems (RED-UAS)*, pp. 351–359, IEEE, 2015.

[17] J. S. Sobolewski, *Cyclic Redundancy Check*, p. 476–479. John Wiley and Sons Ltd., 2003.